Geomech. Geophys. Geo-energ. Geo-resour. (2023) 9:150
https://doi.org/10.1007/s40948-023-00688-z

RESEARCH

Theoretical analysis of anchorage-seepage coupling effect of the surrounding rock stability in deep buried abandoned chambers

Zenghui Zhao · Canlin Li · Zhe Meng · Hao Liu

Received: 23 August 2023 / Accepted: 1 November 2023

Abstract How to ensure the safety of abandoned mine resources, scientifically develop and utilize abandoned mine resources, and promote the transformation of resource-exhausted mining areas have become an important issue in the field of energy and environment in the world today. Aiming at the stability of the surrounding rock in deep closed/abandoned mine chamber, the mechanical model of the surrounding rock under the coupling effect of anchorage and seepage field was proposed. Considering the elastic brittleness degradation and plastic dilatancy effect of rock mass, the analytical solutions of stress and displacement of rockbolt-seepage-surrounding rock coupling system were respectively deduced, and the accuracy of the results were verified. Based on the analytical results, the evolution law of stress and displacement of the surrounding rock under the combined action of seepage field and anchorage effect were further revealed, and a new quantitative design method of rockbolt parameters was proposed. Results show that the influence of rockbolt spacing and rod diameter on the mechanical field is obvious, while the rockbolt length and pre-tension load is small. Dense, short rockbolt with larger diameter should be used in the surrounding rock of deep chamber. The influence of seepage on the displacement of the surrounding rock is very significant. The more serious the seepage is, the more obvious the control effect of rockbolt on the displacement is. Appropriately increasing the density and diameter of rockbolt can effectively reduce the displacement of the surrounding rock.

Z. Zhao (✉) · C. Li · Z. Meng · H. Liu
College of Energy and Mining Engineering, Shandong University of Science and Technology, Qingdao 266590, China
e-mail: tgzyzzh@163.com

Z. Zhao
State Key Laboratory of Mining Disaster Prevention and Control Co-Founded By Shandong Province and the Ministry of Science and Technology, Shandong University of Science and Technology, Qingdao 266590, China

Article Highlights

(1) Closed analytical solutions of stress and displacement in deep buried abandoned chamber under the coupling effect of anchorage-seepage are respectively derived.
(2) The influence of rockbolt parameters and seepage field on the stress and displacement field of the surrounding rock is revealed.
(3) A new quantitative design method of rockbolt parameters is proposed.

Keywords Abandoned chamber · Anchorage-seepage coupling effect · Pre-tension load · Analytical solution

List of symbols

p_0	Hydrostatic stress
p_i	Internal pressure at chamber wall
r_i	Radius of the chamber
r_b	Radius of plastic bolted zone
r_p	Radius of plastic non-bolted zone
S_c	Circumferential spacing of rockbolt
S_l	Longitudinal spacing of rockbolt
L_b	Length of rockbolt
d_b	Diameter of rockbolt
E	Elastic modulus of the surrounding rock
μ	Poisson's ratio of the surrounding rock
σ_r	Radial stress
σ_θ	Circumferential stress
ε_r	Radial strain
ε_θ	Circumferential strain
r	Radial distance from the center of the chamber
u	Radial displacement
σ_1	Major principal stress
σ_3	Minor principal stress
ε_1	Major principal strain
ε_3	Minor principal strain
η	Material constant for Mohr–Coulomb rock mass
ξ	Material constant for Mohr–Coulomb rock mass
c	Cohesion of the surrounding rock
φ	Internal friction angle of the surrounding rock
Ψ	Dilation angle of the surrounding rock
Θ	Dilation coefficient
H	Total water head at r
h_i	Water head at r_i
h_b	Water head at r_b
Δh	Water head difference between r_i and r_b
γ_w	Unit weight of water
K	Equivalent pore water pressure coefficient of rock
σ_r'	Total radial stress of the surrounding rock after applying the rockbolt
A_b	Cross-sectional area of the rockbolt
E_b	Elastic modulus of the rockbolt
ε_b	Axial strain of the rockbolt
C	Arrangement density of the rockbolt
F_b	Pre-tension load
ε_t	Axial strain of the rockbolt generated by pre-tension load
u_p'	Radial displacement of the plastic zone before applying the rockbolt
Superscript e	Elastic part of strain
Superscript p	Plastic part of strain
Subscript e	Refers to quantities corresponding to the elastic zone
Subscript p	Refers to quantities corresponding to the plastic non-bolted zone
Subscript b	Refers to quantities corresponding to the plastic bolted zone
Subscript bp	Refers to quantities corresponding at the interface between plastic bolted and non-bolted zone
Subscript pe	Refers to quantities corresponding at elastic–plastic interface
Subscript r	Values of rock mass parameters after strength drop

1 Introduction

Many factors, such as the gradual depletion of shallow coal resources, the structural reform of the energy supply side and the capacity reduction, have led to the closure of China's resource-exhausted and backward production capacity mines. It is expected that by 2030, China's closed mines will reach 15,000, and the resulting coal mine safety production and ecological environment problems in mining areas will become increasingly prominent (Yuan et al. 2018; Salom and Kivinen 2020; Artwell et al. 2021; Mhlongo 2023; Chen et al. 2023). In the context of 'double carbon' strategy, low carbon green sustainable development and circular economy, how to ensure the safety of abandoned mine resources, scientific development and utilization of abandoned mine resources, and promote the transformation of resource-exhausted mining areas has become an important issue in the field of energy and environment in the world (Wang et al. 2021; Yuan and Yang 2021).

At present, many countries have used closed/abandoned mines to store CO_2 and built pumped storage power stations, underground medical research centers, underground sanatoriums and underground shaft parking garages (Cui et al. 2020; Xue et al. 2022; Guo

Fig. 1 Abandoned Bullitt mine in Virginia, USA (Reese 2017)

et al. 2023; Yang et al. 2023). The geological conditions and mining environment of mines in China are complex, and the utilization of closed/abandoned mines is still in its infancy. The deep closed/abandoned mine chamber is affected by high in-situ stress and mine water seepage, and the evolution of mechanical properties of bolted rock is extremely complex, which leads to the hidden instability of chambers and is not conducive to the full life cycle service of chambers. Therefore, it is an important guarantee for the safe utilization of resources in abandoned mines to deeply reveal the multi-field coupling stability mechanism of the surrounding rock in abandoned mines (Fig. 1).

Many scholars have carried out extensive research on the stability of the surrounding rock of circular chambers considering seepage field. The main method is to regard seepage force as volume force. Li et al. (2004), Zareifard and Fahimifar (2015), Huang and Yang (2010) obtained the analytical solution of circular tunnel based on Mohr–Coulomb and Hoek–Brown criteria, respectively. On the basis of seepage, Rong and Cheng (2004), Liu et al. (2009), Zhang et al. (2013) respectively considered the influence of damage, stress redistribution and temperature, and deduced the elastic–plastic solution of circular tunnel. Based on the generalized effective stress principle, Zareifard (2018) gave the elastic analytical solution of pressure tunnel with permeable lining. Most of the above studies have only obtained the stress solution, and the plastic radius needs to be calculated by numerical methods.

For the interaction between rockbolt and rock in the circular chamber, there are mainly the following four treatment methods: the first is simplified to apply uniform pressure on both sides of the bolted zone (Li and Hou 2008; Cai et al. 2020); the second is regarded as the improvement of the surrounding rock parameters of the bolted zone (Osgoui and Oreste 2010); the third is to convert the relative displacement of the rockbolt and the surrounding rock into the force of the rockbolt on the surrounding rock (Cui et al. 2022); the fourth is to regard as increasing the radial stress of the surrounding rock. Among them, many scholars use the fourth method for theoretical analysis. For example, Fahimifar and Soroush (2005) derived the stress and displacement solutions of bolted surrounding rock under elastic-brittle-plastic and strain-softening models based on Hoek–Brown criterion. Zou et al. (2018), Fahimifar and Ranjbarnia (2009) analyzed the stress and displacement of the bolted surrounding rock considering the seepage, the pre-tension load of the rockbolt and the effect of distance of bolted section to tunnel face, respectively. Carranza-Torres (2009) obtained the elastic solutions of the interaction between the grouted and anchored rockbolts and the surrounding rock by using the dimensionless coordinates. The solutions obtained in the above research are all numerical solutions obtained by MATLAB or FDM. Zhao et al. (2016) decomposed the bolted surrounding rock into the initial state model before anchoring and the enhance model after anchoring. The analytical solutions of the above two models were obtained respectively, and then the elastic stress and displacement solutions of the bolted surrounding rock under the original model were obtained by superposition. Based on the strain softening model, Sun et al. (2019) established the interaction model of rockbolt and surrounding rock, and analyzed the whole process, but they did not consider the influence of seepage. Based on the elastic-brittle-plastic model and considering the influence of seepage, Shin et al. (2011) derived the stress solution of the bolted surrounding rock and the displacement of the tunnel surface. However, the elastic strain of the plastic zone is regarded as a constant, which is always equal to the strain on the elastic–plastic boundary, which will underestimate the displacement of the surrounding rock (Park and Kim 2006).

At present, most scholars have carried out theoretical analysis on seepage and bolted rock, respectively. There are few theoretical studies on the coupling of the two, and the analytical solutions obtained are not complete. The stability of the surrounding rock in deep abandoned chamber is related to many factors, such as stress field, seepage field, rockbolt parameters and pre-tension load. The comprehensive effect of these factors on the mechanical properties of bolted rock is still lack of quantitative understanding. In view of this, this paper considers the influence of the coupling effect of anchorage and seepage field. By establishing the mechanical model of rockbolt-rock-seepage, the analytical field of stress and displacement of bolted rock in abandoned chamber is obtained, and the quantitative characterization of the influence law of pre-tension load and seepage force is realized.

2 Rockbolt-rock-seepage mechanical model in deep chamber

2.1 Definition of the problem

In order to obtain the analytical solution, the section of the deep mine chamber is simplified into a circle. After the excavation of the chamber, the surrounding rock will deteriorate rapidly due to the unloading effect, and the elastic zone and the plastic zone will be generated. For the deep rock mass, the strength of the disturbed surrounding rock is obviously degraded. After the rockbolt is applied to the chamber, the surrounding rock will form plastic bolted zone (PBZ), plastic non-bolted zone (PNZ) and elastic zone (EZ), as shown in Fig. 2. The surrounding rock of the chamber is subjected to a hydrostatic pressure p_0, the internal pressure at the chamber wall is p_i, the radii of chamber, plastic bolted and non-bolted zone are r_i, r_b and r_p, respectively. The circumferential and longitudinal spacing of rockbolt are S_c and S_l. The length and diameter of rockbolt are $L_b = r_b - r_i$ and d_b.

For the convenience of analysis, the following assumptions are made: (1) Without considering the influence of the surrounding rock weight, the problem is regarded as a plane strain problem. (2) The rockbolt is applied to the plastic zone. (3) Because the seepage has little effect on the distant surrounding rock, the seepage effect is only considered in the PBZ. (4) The rockbolt is elastic material. The EZ can be analyzed by Lame's solution (Xu 2016), and the PNZ is analyzed by the stress drop model.

2.2 Elastic–plastic constitutive and strength criterion

By assuming that the compressive stress is taken positive and the tensile stress is taken negative. Only considering the displacement caused by excavation, the constitutive of the EZ can be written as

$$\begin{aligned} \varepsilon_{re} &= \frac{1-\mu^2}{E}\left[\left(\sigma_{re}-p_0\right)-\frac{\mu}{1-\mu}\left(\sigma_{\theta e}-p_0\right)\right] \\ \varepsilon_{\theta e} &= \frac{1-\mu^2}{E}\left[\left(\sigma_{\theta e}-p_0\right)-\frac{\mu}{1-\mu}\left(\sigma_{re}-p_0\right)\right] \end{aligned} \tag{1}$$

where E and μ are elastic modulus and Poisson's ratio of rock mass, σ_r and σ_θ are stresses in the radial and

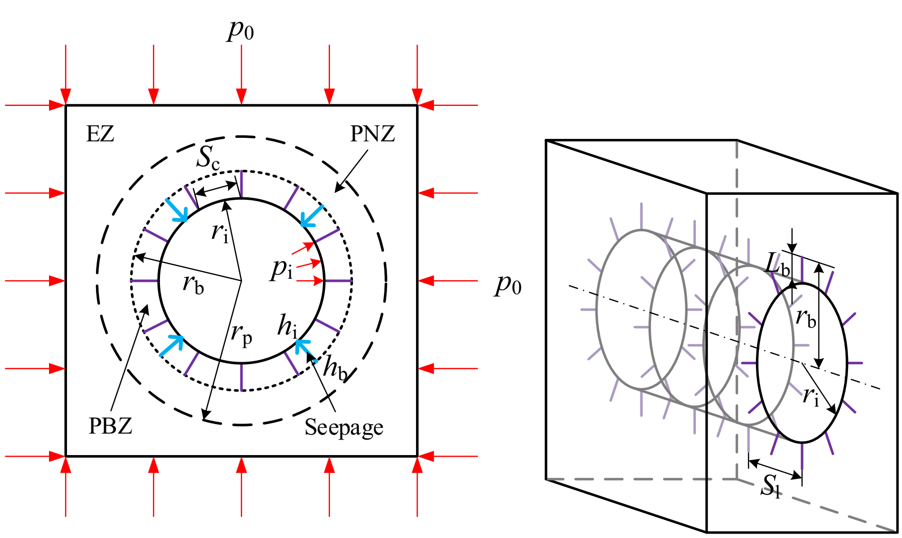

Fig. 2 Mechanical model of rockbolt-rock interaction in deep mine chamber

circumferential directions, ε_r and ε_θ are strains in the radial and circumferential directions, the subscript e represents EZ.

The equilibrium differential equation of axisymmetric plane problem can be simplified as

$$\frac{d\sigma_r}{dr} + \frac{\sigma_r - \sigma_\theta}{r} = 0 \tag{2}$$

The geometric equation is

$$\varepsilon_r = \frac{du}{dr},\ \varepsilon_\theta = \frac{u}{r} \tag{3}$$

where u is radical displacement.

The Mohr–Coulomb criterion is used to describe the strength characteristics of the surrounding rock. Due to the axial symmetry of the problem, it is assumed that the stress in the axial direction of the chamber is the intermediate principal stress, then the principal stress $\sigma_1=\sigma_\theta$, $\sigma_3=\sigma_r$, the principal strain $\varepsilon_1=\varepsilon_\theta$, $\varepsilon_3=\varepsilon_r$. As shown in Fig. 3a, the peak strength at point A is

$$\sigma_\theta = \eta\sigma_r + \xi \tag{4}$$

where $\eta=\frac{1+\sin\varphi}{1-\sin\varphi}$, $\xi=\frac{2c\cos\varphi}{1-\sin\varphi}$, c and φ are the cohesion and internal friction angle of the surrounding rock, respectively.

After the strength drops to point B, the postpeak residual strength of PNZ is

$$\sigma_\theta = \eta_r\sigma_r + \xi_r \tag{5}$$

where $\eta_r=\frac{1+\sin\varphi_r}{1-\sin\varphi_r}$, $\xi_r=\frac{2c_r\cos\varphi_r}{1-\sin\varphi_r}$, the subscript r represents the residual stage.

The strain of PNZ can be decomposed into

$$\begin{aligned} \varepsilon_{rp} &= \varepsilon_{rp}^{e} + \varepsilon_{rp}^{p} \\ \varepsilon_{\theta p} &= \varepsilon_{\theta p}^{e} + \varepsilon_{\theta p}^{p} \end{aligned} \tag{6}$$

where the superscripts e and p represent elastic strain and plastic strain respectively, and the subscript p represents PNZ.

The elastic strain of the PNZ satisfies Hooke's law, it should be written as

$$\begin{aligned} \varepsilon_{rp}^{e} &= \frac{1-\mu_r^2}{E}\left[\left(\sigma_{rp}-p_0\right) - \frac{\mu_r}{1-\mu_r}\left(\sigma_{\theta p}-p_0\right)\right] \\ \varepsilon_{\theta p}^{e} &= \frac{1-\mu_r^2}{E_r}\left[\left(\sigma_{\theta p}-p_0\right) - \frac{\mu_r}{1-\mu_r}\left(\sigma_{rp}-p_0\right)\right] \end{aligned} \tag{7}$$

By assuming that the plastic strain in the PNZ obeys the non-associated flow rule, as shown in Fig. 3b, then the plastic strain in the PNZ satisfies

$$\varepsilon_{rp}^{p} + \Theta\varepsilon_{\theta p}^{p} = 0 \tag{8}$$

where $\Theta=(1+\sin\Psi)/(1-\sin\Psi)$, Ψ is the dilation angle of the surrounding rock. For the PBZ, the subscript p in Eqs. (6)–(8) is replaced by b to represent the corresponding amount of the PBZ.

2.3 Seepage force

The axisymmetric steady seepage equation is (Yuan et al. 2001)

$$\nabla^2 H = \frac{\partial^2 H}{\partial r^2} + \frac{1}{r}\frac{\partial H}{\partial r} = 0 \tag{9}$$

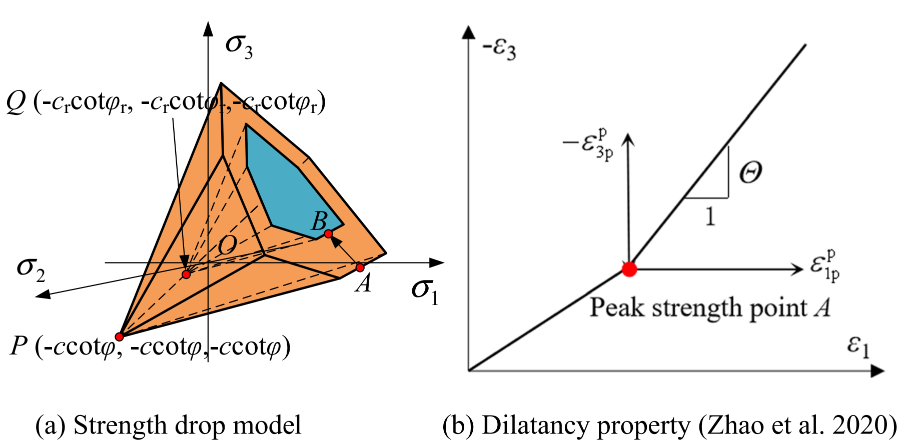

Fig. 3 Strength and deformation characteristics of the surrounding rock in plastic region

where H is the total water head at r.

Considering the boundary conditions when $r=r_i$, $H=h_i$; $r=r_b$, $H=h_b$, the seepage field can be obtained as

$$H = \frac{h_b - h_i}{\ln\left(r_b/r_i\right)} \ln\frac{r}{r_i} + h_i \tag{10}$$

The seepage force is regarded as volume force, and let $\Delta h=h_b$-h_i. Combined with Eq. (10), Eq. (2) can be rewritten as (Li et al. 2004):

$$\frac{d\sigma_r}{dr} + \frac{\sigma_r - \sigma_\theta}{r} + \frac{\gamma_w K \Delta h}{r\ln\left(r_b/r_i\right)} = 0 \tag{11}$$

where γ_w is the unit weight of water, and K is the equivalent pore water pressure coefficient of rock.

2.4 Rockbolt-rock interaction

The effect of the rockbolt on the surrounding rock is equivalent to applying a radial constraint force in the rock mass (Huang et al. 2002), so the total radial stress of the surrounding rock after applying the rockbolt is (Fahimifar and Ranjbarnia 2009):

$$\sigma_r' = \sigma_r - A_b E_b \varepsilon_b C \tag{12}$$

where A_b, E_b, ε_b and C are the cross-sectional area, elastic modulus, axial strain and arrangement density of the rockbolt, respectively, and $C=1/(S_c S_l)$.

Considering the influence of pre-tension load F_b, the axial strain of the rockbolt is

$$\varepsilon_b = \varepsilon_r + \varepsilon_t \tag{13}$$

where $\varepsilon_t = \frac{F_b}{A_b E_b}$ is axial strain generated by pre-tension load.

By substituting Eq. (13) into Eq. (12), we can get

$$\sigma_r' = \sigma_r - A_b E_b \varepsilon_r C - F_b C \tag{14}$$

Therefore, the equilibrium differential equation of PBZ is

$$\frac{d\sigma_r'}{dr} + \frac{\sigma_r' - \sigma_\theta}{r} + \frac{\gamma_w K \Delta h}{r\ln\left(r_b/r_i\right)} = 0 \tag{15}$$

The strength criterion of PBZ is

$$\sigma_\theta = \eta_r \sigma_r' + \xi_r \tag{16}$$

3 Analytical solution of stress and displacement of the surrounding rock

3.1 Stress solution

3.1.1 Plastic bolted zone

The radial displacement of the plastic zone before the surrounding rock is applied to the rockbolt is (Park and Kim 2006).

$$u_p' = k_1\left(r - r_p'\right) + \frac{k_2}{\eta_r}\left(r^{\eta_r} - r_p'^{\eta_r}\right) - \frac{k_3}{\Theta} r^{-\Theta} \tag{17}$$

where $k_1 = \frac{(1+\mu_r)(1-2\mu_r)}{E_r}\left(\frac{\xi_r}{1-\eta_r} - p_0\right)$,

$k_2 = \frac{(1+\mu_r)[(1-\mu_r-\Theta\mu_r)+\eta_r(\Theta-\Theta\mu_r-\mu_r)]}{E_r}\left(p_i + \frac{\xi_r}{\eta_r-1}\right)\frac{\eta_r r_i^{1-\eta_r}}{\Theta+\eta_r}$,

$k_3 = -\Theta u_{pe}' r_p'^{\Theta}$.

By substituting Eq. (17) into Eq. (3), the radial strain in the plastic zone can be obtained as

$$\varepsilon_r = k_1 + k_2 r^{\eta_r - 1} + k_3 r^{-(\Theta+1)} \tag{18}$$

Combining Eqs. (14)–(16) and (18), and using the boundary condition $r=r_i$, $\sigma_r=p_i$, the stress solution in the PBZ can be obtained as

$$\begin{aligned} \sigma_{rb} &= k_3 k_4 r^{-(\Theta+1)} + k_6 r^{\eta_r-1} + k_7 \\ \sigma_{\theta b} &= \eta_r\left(k_6 - k_2 k_4\right) r^{\eta_r-1} + \frac{\xi_r - \eta_r k_5}{1-\eta_r} \end{aligned} \tag{19}$$

where $k_4 = A_b E_b C$, $k_5 = \frac{\gamma_w K \Delta h}{\ln\left(r_b/r_i\right)}$,

$k_6 = \left(p_i - k_3 k_4 r_i^{-(\Theta+1)} - k_1 k_4 - F_b C + \frac{k_5-\xi_r}{1-\eta_r}\right) r_i^{1-\eta_r}$,

$k_7 = k_1 k_4 + F_b C - \frac{k_5-\xi_r}{1-\eta_r}$.

By substituting $r=r_b$ into Eq. (19), the radial stress at the interface between plastic bolted and non-bolted zone can be obtained as

$$\sigma_{rbp} = k_3 k_4 r_b^{-(\Theta+1)} + k_6 r_b^{\eta_r-1} + k_7 \tag{20}$$

3.1.2 Plastic non-bolted zone

By substituting Eq. (5) into Eq. (2), and using the boundary condition $r=r_b$, $\sigma_r=\sigma_{rbp}$, the stress solution in the PNZ can be obtained as

$$\begin{aligned}\sigma_{rp} &= \left(\sigma_{rbp}+\frac{\xi_r}{\eta_r-1}\right)\left(\frac{r}{r_b}\right)^{\eta_r-1}-\frac{\xi_r}{\eta_r-1}\\ \sigma_{\theta p} &= \eta_r\left(\sigma_{rbp}+\frac{\xi_r}{\eta_r-1}\right)\left(\frac{r}{r_b}\right)^{\eta_r-1}-\frac{\xi_r}{\eta_r-1}\end{aligned} \tag{21}$$

At the elastic–plastic interface, the stress should satisfy $\sigma_{rpe}+\sigma_{\theta pe}=2p_0$, by substituting it into Eq. (4), and the radial stress at the elastic–plastic interface can be obtained as

$$\sigma_{rpe}=\frac{2p_0-\xi}{\eta+1} \tag{22}$$

By using $r=r_p$, $\sigma_r=\sigma_{rpe}$ in Eq. (19), the plastic radius can be obtained as the plastic radius can be obtained as

$$r_p=\left\{\frac{(\eta_r-1)(2p_0-\xi)+(\eta+1)\xi_r}{(\eta+1)\left[(\eta_r-1)\sigma_{rbp}+\xi_r\right]}\right\}^{\frac{1}{\eta_r-1}}r_b \tag{23}$$

3.1.3 Elastic zone

By using Lame's solution and the boundary conditions $r=r_p$, $\sigma_r=\sigma_{rpe}$; $r\to\infty$, $\sigma_r=p_0$, the stress solution in the EZ can be obtained as

$$\begin{aligned}\sigma_{re} &= \left[1-\left(\frac{r_p}{r}\right)^2\right]p_0+\left(\frac{r_p}{r}\right)^2\sigma_{rpe}\\ \sigma_{\theta e} &= \left[1+\left(\frac{r_p}{r}\right)^2\right]p_0-\left(\frac{r_p}{r}\right)^2\sigma_{rpe}\end{aligned} \tag{24}$$

3.2 Displacement solution

3.2.1 Elastic zone

Combining Eqs. (1), (3) and (24), and using the boundary condition $t\to\infty$, $u_e\to 0$, the EZ displacement can be obtained

$$u_e=\frac{1+\mu}{E}\left(p_0-\sigma_{rpe}\right)\frac{r_p^2}{r} \tag{25}$$

By substituting $r=r_p$ in Eq. (25), the displacement at the elastic–plastic interface can be obtained as

$$u_{pe}=\frac{1+\mu}{E}\left(p_0-\sigma_{rpe}\right)r_p \tag{26}$$

3.2.2 Plastic non-bolted zone

By substituting Eqs. (3) and (7) into Eq. (6), and then substituting the resulting expression in Eq. (8), the differential equation for the displacement in the PNZ may be written as (Zhao et al. 2023)

$$\frac{du_p}{dr}+\Theta\frac{u_p}{r}=f(r) \tag{27}$$

where $f(r)=\frac{1+\mu_r}{E_r}\{[1-(\Theta+1)\mu_r]\sigma_{rp}+[\Theta-(\Theta+1)\mu_r]\sigma_{\theta p}-(\Theta+1)(1-2\mu_r)p_0\}$.

By using the boundary condition $r=r_p$, $u=u_{pe}$, and then solving Eq. (27), the displacement in the PNZ can be obtained as

$$u_p=r^{-\Theta}\int_{r_p}^{r}r^{\Theta}f(r)dr+u_{pe}\left(\frac{r_p}{r}\right)^{\Theta} \tag{28}$$

By integrating the above equation, the displacement in the PNZ can be obtained as

$$\begin{aligned}u_p &= \frac{1+\mu_r}{E_r}\frac{1}{r^{\Theta}}\left[A_1\left(r^{\Theta+\eta_r}-r_p^{\Theta+\eta_r}\right)\right.\\ &\left.+A_2\left(r^{\Theta+1}-r_p^{\Theta+1}\right)\right]+u_{pe}\left(\frac{r_p}{r}\right)^{\Theta}\end{aligned} \tag{29}$$

where $A_1=\left[1-(\Theta+1)\mu_r+\eta_r\Theta-\eta_r(\Theta+1)\mu_r\right]\frac{1}{\Theta+\eta_r}\left(\sigma_{rbp}+\frac{\xi_r}{\eta_r-1}\right)r_b^{1-\eta_r}$,

$A_2=-(1-2\mu_r)\left(\frac{\xi_r}{\eta_r-1}+p_0\right)$.

By substituting $r=r_b$ in Eq. (29), the displacement at the interface between plastic bolted and non-bolted zone can be obtained as

$$\begin{aligned}u_{bp} &= \frac{1+\mu_r}{E_r}\frac{1}{r_b^{\Theta}}\left[A_1\left(r_b^{\Theta+\eta_r}-r_p^{\Theta+\eta_r}\right)\right.\\ &\left.+A_2\left(r_b^{\Theta+1}-r_p^{\Theta+1}\right)\right]+u_{pe}\left(\frac{r_p}{r_b}\right)^{\Theta}\end{aligned} \tag{30}$$

3.2.3 Plastic bolted zone

In the same way, the differential equation for the displacement in the PBZ may be written as

$$\frac{du_b}{dr}+\Theta\frac{u_b}{r}=f(r) \tag{31}$$

where $f(r)=\frac{1+\mu_r}{E_r}\left\{\left[1-(\Theta+1)\mu_r\right]\sigma_{rb}+\left[\Theta-(\Theta+1)\mu_r\right]\sigma_{\theta b}-(\Theta+1)(1-2\mu_r)p_0\right\}$.

Based on the boundary condition $r=r_b$, $u=u_{bp}$, the displacement in the PBZ can be obtained from Eq. (31)

$$u_b=r^{-\Theta}\int_{r_b}^{r} r^{\Theta}f(r)dr+u_{bp}\left(\frac{r_b}{r}\right)^{\Theta} \tag{32}$$

By substituting Eq. (19) into Eq. (32), the displacement in the PBZ can be obtained as

$$u_b=\frac{1+\mu_r}{E_r}\frac{1}{r^{\Theta}}\left[A_3\ln\frac{r}{r_b}+A_4\left(r^{\Theta+\eta_r}-r_b^{\Theta+\eta_r}\right)+A_5\left(r^{\Theta+1}-r_b^{\Theta+1}\right)\right]+u_{bp}\left(\frac{r_b}{r}\right)^{\Theta} \tag{33}$$

where $A_3=\left[1-(\Theta+1)\mu_r\right]k_3k_4$, $A_4=\left\{\left[1-(\Theta+1)\mu_r\right]k_6+\left[\Theta-(\Theta+1)\mu_r\right]\eta_r\left(k_6-k_2k_4\right)\right\}\frac{1}{\Theta+\eta_r}$,

$A_5=\left\{\left[1-(\Theta+1)\mu_r\right]k_7+\left[\Theta-(\Theta+1)\mu_r\right]\frac{\xi_r-\eta_r k_5}{1-\eta_r}\right\}\frac{1}{\Theta+1}-(1-2\mu_r)p_0$.

By substituting $r=r_i$ in Eq. (33), the displacement at the chamber wall can be obtained as

$$u_i=\frac{1+\mu_r}{E_r}\frac{1}{r_i^{\Theta}}\left[A_3\ln\frac{r_i}{r_b}+A_4\left(r_i^{\Theta+\eta_r}-r_b^{\Theta+\eta_r}\right)+A_5\left(r_i^{\Theta+1}-r_b^{\Theta+1}\right)\right]+u_{bp}\left(\frac{r_b}{r_i}\right)^{\Theta} \tag{34}$$

4 Model validation

In order to verify the correctness of the analytical solution in this paper, the analytical solution is compared with the numerical solution of Zou et al. (2018). The parameter values are shown in Tables 1 and 2 (Zou et al. 2018). In this paper, it is assumed that the rockbolt is located in the plastic zone, and the rockbolt end in Zou et al. (2018) is located at elastic–plastic interface, so we let $r_b=r_p$. The drop of elastic modulus and Poisson's ratio in plastic zone and the influence of pre-tension load are not considered in Zou et al. (2018). The comparison results are shown in Fig. 4, and the analytical results are very close to the numerical solution of Zou et al. (2018), which shows the correctness of the analytical results in this paper. In addition, this paper considers the elastic modulus drop, pre-tension load, rockbolt length and seepage, etc., which can comprehensively analyze the influence of various factors on the stability of the surrounding rock.

Table 2 Rockbolt, chamber and seepage field parameters

Rockbolt		Chamber		Seepage field	
E_b/GPa	200	r_i/m	2.0	γ_w/(kN/m)	10
d_b/mm	25	p_i/MPa	6.5	K	1
S_c、S_l/m	0.79	P_0/MPa	50.0	Δh/m	100
F_b/kN	0				

5 Influence of different factors on the mechanical field of bolted rock

Taking the calculation parameters shown in Tables 3 and 4 as the basic data, the influence of different seepage forces and rockbolt parameters on the stress and displacement field of the surrounding rock is further analyzed.

5.1 Influence of seepage field

According to Eqs. (19), (21) and (24), Fig. 5 shows the stress change trend of the surrounding rock with different water head difference Δh. In the PBZ, the circumferential stress and the radial stress after rockbolting should meet the M-C criterion, while in the PNZ, the circumferential stress and the radial stress before rockbolting should also meet the M-C criterion, so the circumferential stress at the interface between the two zones has a sudden change. Due to

Table 1 Surrounding rock parameters

E/GPa	E_r/GPa	μ	μ_r	c/MPa	c_r/MPa	φ/°	φ_r/°	Ψ/°
11	11	0.24	0.24	1.68	1.0	33.21	26.23	0

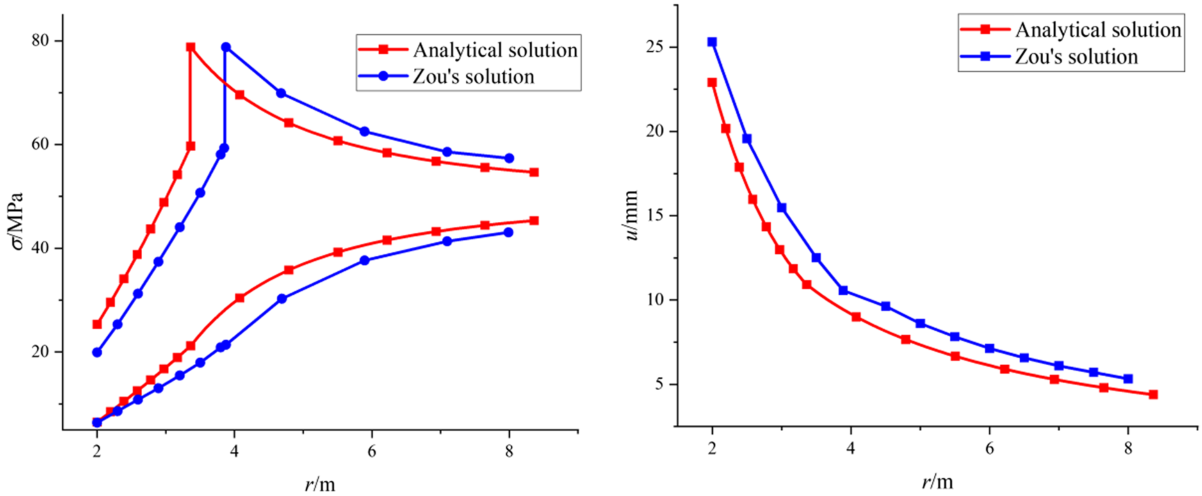

(a) Stress comparison (b) Displacement comparison

Fig. 4 Result comparison of proposed method with Zou et al. (2018)

Table 3 Surrounding rock parameters

E/GPa	E_r/GPa	μ	μ_r	c/MPa	c_r/MPa	φ/°	φ_r/°	Ψ/°
11	5	0.24	0.24	1.68	1.0	33.21	26.23	11.74

Table 4 Rockbolt, chamber and seepage field parameters

Rockbolt		Chamber		Seepage field	
E_b/GPa	210	r_i/m	7.0	γ_w/(kN/m)	9.8
d_b/mm	22	p_i/MPa	1.0	K	1
S_c、S_l/m	0.87	P_0/MPa	10.0	Δh/m	50
F_b/kN	100				
L_b/m	1.0				

the influence of the strength drop in the plastic zone, the circumferential stress at the interface of the elastic–plastic zone also changes abruptly. The boundary conditions taken in this paper are $r = r_i$, $\sigma_r = p_i$, and the stress adjustment after rockbolting is also independent of seepage. Therefore, the stress at the chamber wall is independent of the water head difference and is always constant. According to Eq. (19), when $p_i < \sigma_r^{bp}$, the stress of PBZ decreases with increasing radius, while when $p_i > \sigma_r^{bp}$, the stress increases with increasing radius. With increasing water head difference, the stress in plastic bolted, non-bolted zone and radial stress in EZ decrease. Because the sum of

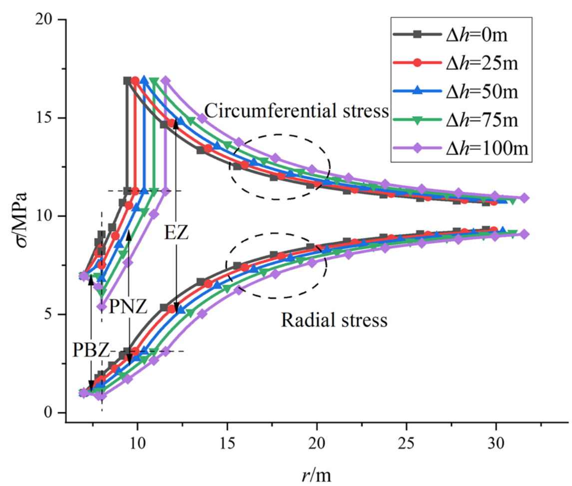

Fig. 5 Stress comparison with different water head difference

radial stress and circumferential stress in EZ is $2p_0$, the circumferential stress in EZ increases.

According to Eqs. (25), (29) and (33), the displacement of the surrounding rock with different

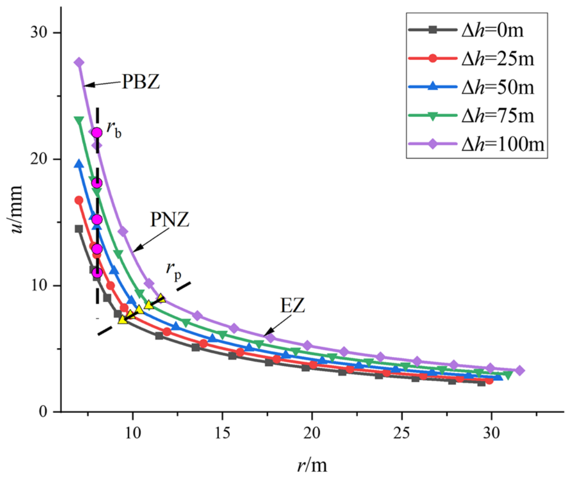

Fig. 6 Displacement comparison with different water head difference

water head difference Δh can be obtained, as shown in Fig. 6. Due to increasing water head difference Δh, the seepage force increases, which leads to the displacement of the surrounding rock and plastic radius increase. For every 25 m increase in the water head difference, the displacement at the chamber wall increases by 15.75%, 16.83%, 18.08% and 19.59%, respectively, and the plastic radius increases by 0.44 m, 0.49 m, 0.56 m and 0.64 m, respectively. It can be seen that the greater the water head difference, the greater the increase of the displacement of the surrounding rock and the plastic radius.

5.2 Influence of rockbolt parameters

In order to reuse the abandoned chamber, it is necessary to quantitatively analyze the matching relationship between rockbolt parameters and surrounding rock displacement with different water head differences, and re-design the rockbolt parameters. According to the national standard of China (GB/T 35056-2018), 18 kinds of rockbolt support examples are compared and studied as shown in Table 5, and the remaining parameters are the same as those in Tables 3 and 4.

Figure 7 is the ground response curve (GRC) with different rockbolt parameters obtained by using Eq. (34). The circumferential and longitudinal spacing of the rockbolt have a significant influence on the displacement of the surrounding rock, the rockbolt diameter has a more obvious influence, and the rockbolt length and the pre-tension load have less influence. The displacement of the surrounding rock decreases with increasing rockbolt diameter, increases with increasing circumferential and longitudinal spacing of rockbolt, and decreases slightly with increasing rockbolt length and pre-tension load. Therefore, when optimizing the rockbolt parameters, the rockbolt spacing should be given priority, followed by the rockbolt diameter, and finally the rockbolt length and the pre-tension load should be considered. Meanwhile, it can be seen from Fig. 7a–d that as the internal pressure at the chamber wall gradually decreases, the influence of rockbolt parameters on the displacement of the surrounding rock becomes more and more obvious. When the water head difference changes from 10 to 100 m, the displacement at the chamber wall becomes about 2 times of the original, indicating that the more serious the seepage is, the greater the influence of the rockbolt parameters on the displacement is, and the better the effect of improving the rockbolt parameters on reducing the displacement at the chamber wall is.

Table 5 Rockbolt parameters of examples

Example	Δh/m	d_b/mm	$S_c = S_l$/m	F_b/kN	L_b/m
1	10	20	1	100	1.8
2		16	1	100	1.8
3		24	1	100	1.8
4		20	0.6	100	1.8
5		20	1.4	100	1.8
6		20	1	50	1.8
7		20	1	150	1.8
8		20	1	100	1.6
9		20	1	100	2.0
10	100	20	1	100	1.8
11		16	1	100	1.8
12		24	1	100	1.8
13		20	0.6	100	1.8
14		20	1.4	100	1.8
15		20	1	50	1.8
16		20	1	150	1.8
17		20	1	100	1.6
18		20	1	100	2.0

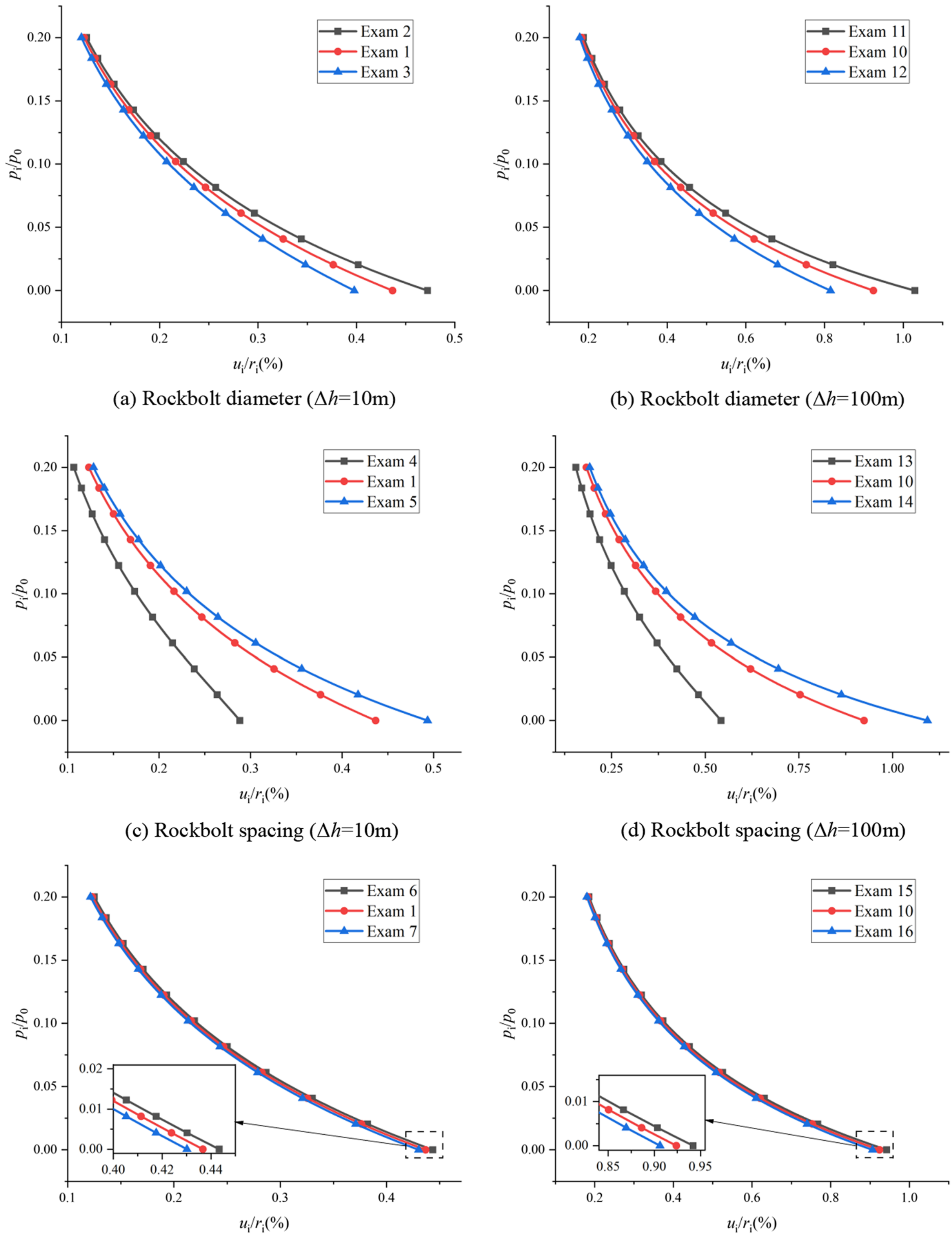

(a) Rockbolt diameter (Δh=10m) (b) Rockbolt diameter (Δh=100m)

(c) Rockbolt spacing (Δh=10m) (d) Rockbolt spacing (Δh=100m)

(e) Pre-tension load (Δh=10m) (f) Pre-tension load (Δh=100m)

Fig. 7 Ground response curve with different rockbolt parameters

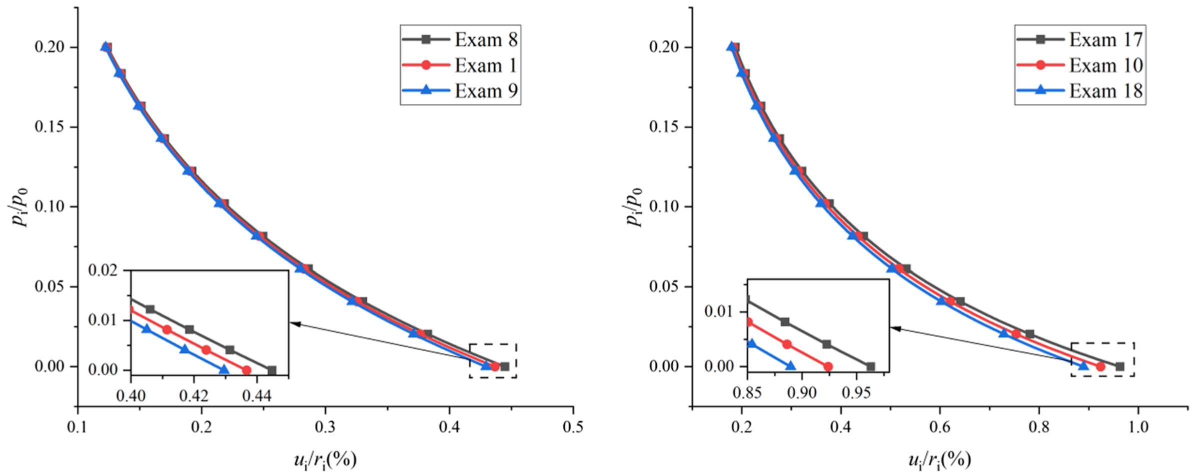

(g) Rockbolt length (Δh=10m)

(h) Rockbolt length (Δh=100m)

Fig. 7 (continued)

5.3 Rockbolt parameters design method based on analytical solution

The following example is given to illustrate the method of using the analytical solution in this paper to design the rockbolt parameters. Taking the calculation parameters shown in Tables 3 and 4, according to the relevant provisions the national standard of China (TB 10003-2005) on the displacement, the allowable displacement at the chamber wall can be calculated as $[u_i]=40$ mm. If the rockbolt is not applied, that is, $d_b=0$ mm, $F_b=0$ kN, according to Eq. (34), the maximum displacement at the chamber wall can be calculated as $u_{max}=57.3$ mm. In order to control the displacement to satisfy the allowable displacement $[u_i]$, according to Eq. (34), the reasonable rockbolt parameters are calculated as $d_b=18$ mm, $S_c=S_l=0.8$ m, $F_b=100$ kN, $L_b=1.6$ m, and the displacement of the chamber wall is $u_i=39.3$ mm $<[u_i]$. Through the above method, the cost can be reduced and the bolted effect can be improved, which has certain guiding significance for the selection and arrangement of rockbolt.

6 Conclusion

Aiming at the problem of multi-field coupling of rockbolt-rock-seepage in closed/abandoned mine chamber, the analytical solution of stress and displacement of bolted rock in chamber is deduced, and the influence of water head difference and rockbolt parameters on the stress and displacement of the surrounding rock is revealed. The main conclusions are as follows:

(1) The rockbolt spacing and diameter have a significant influence on the displacement of the surrounding rock, and the influence of pre-tension load is less. Because the deformation of the surrounding rock far away from the chamber wall is small, the strain of the rockbolt end is not large, so the rockbolt length has little effect on the displacement of the surrounding rock. Therefore, when the deep abandoned chamber is reused, the dense, short and thick rockbolt should be used as far as possible.

(2) The seepage field has a significant effect on the stress and displacement of the bolted rock. The larger the water head difference, the smaller the stress of the plastic bolted and non-bolted zone and the radial stress of the EZ, and the larger the radius and displacement of the plastic zone. In the case of serious seepage, the displacement control of the surrounding rock by rockbolt is more significant. Appropriate increase of rockbolt density and diameter can effectively reduce the displacement of the surrounding rock.

(3) The analytical results realize the quantitative characterization of rockbolt parameters, stress field, physical and mechanical parameters of the surrounding rock. The design method of rockbolt parameters based on analytical method has important theoretical guiding significance for optimizing the rockbolt configuration of abandoned mines.

Author contribution ZZ Conceptualization, Methodology, Funding acquisition and Supervision. LC Theoretical analysis, Writing—original draft, Reviewing the manuscript. MZ and LH Reviewing the manuscript.

Funding This project is supported by National Natural Science Foundation of China (Grant No. 51774196) and Natural Science Foundation of Shandong Province (No. ZR2023ME086).

Data availability All the data, models or code generated or used in the present study are available from the corresponding author by request.

Declarations

Ethics approval and consent to participate The authors declare that this paper does not involve ethical issues.

Consent to Publish All authors consent to submit the paper to Geomechanics and Geophysics for Geo-Energy and Geo-Resources.

Competing interests The authors declare that they have no known competing financial interests or personal relationships that could have appeared to influence the work reported in this paper.

References

Artwell K, France N, Peter M (2021) Trace elements in groundwater near an abandoned mine tailings dam and health risk assessment (ne zimbabwe). Water SA. https://doi.org/10.17159/wsa/2021.v47.i4.3851

Cai H, Lu AZ, Ma YC (2020) An analytical solution for shallow buried tunnel reinforced by point anchored rockbolts. Tunn Undergr Space Technol 100:103402. https://doi.org/10.1016/j.tust.2020.103402

Carranza-Torres C (2009) Analytical and numerical study of the mechanics of rockbolt reinforcement around tunnels in rock masses. Rock Mech Rock Eng 42(2):175–228. https://doi.org/10.1007/s00603-009-0178-2

Chen BQ, Liu H, Li ZH, Zheng MN, Yu Y, Yu H, Qin L, Yang JL, Yang Y (2023) Research progress and prospect of secondary subsidence monitoring, prediction and stability evaluation in closed underground mines. J China Coal Soc 48(2):943–958. https://doi.org/10.13225/j.cnki.jccs.2022.1385. (**in Chinese**)

Cui CQ, Wang B, Zhao YX, Xue LM (2020) Waste mine to emerging wealth: Innovative solutions for abandoned underground coal mine reutilization on a waste management level. J Clean Prod 252:119748. https://doi.org/10.1016/j.jclepro.2019.119748

Cui L, Sheng Q, Dong YK, Xie MX (2022) Unified elasto-plastic analysis of rock mass supported with fully grouted bolts for deep tunnels. Int J Numer Anal Methods Geomech 46(2):247–271. https://doi.org/10.1002/nag.3298

Fahimifar A, Ranjbarnia M (2009) Analytical approach for the design of active grouted rockbolts in tunnel stability based on convergence-confinement method. Tunn Undergr Space Technol 24(4):363–375. https://doi.org/10.1016/j.tust.2008.10.005

Fahimifar A, Soroush H (2005) A theoretical approach for analysis of the interaction between grouted rockbolts and rock masses. Tunn Undergr Space Technol 20(4):333–343. https://doi.org/10.1016/j.tust.2004.12.005

Guo P, Wang M, Dang G, Zhu T, Wang J, He M (2023) Evaluation method of underground water storage space and thermal reservoir model in abandoned mine. Rock Mech Bull 2(2):100044. https://doi.org/10.1016/j.rockmb.2023.100044

Huang F, Yang XL (2010) Analytical solution of circular openings subjected to seepage in Hoek-Brown media. Rock Soil Mech 31(5):1627–1632. https://doi.org/10.16285/j.rsm.2010.05.013. (**in Chinese**)

Huang Z, Broch E, Lu M (2002) Cavern roof stability—mechanism of arching and stabilization by rockbolting. Tunn Undergr Space Technol 17(3):249–261. https://doi.org/10.1016/S0886-7798(02)00010-X

Li DW, Hou CJ (2008) Calculation of bolt support in surrounding rock strain softening roadway. J Min Saf Eng 25(1):123–126 (**in Chinese**)

Li ZL, Ren QW, Wang YH (2004) Elasto-plastic analytical solution of deep-buried circle tunnel considering fluid flow field. Chin J Rock Mech Eng 23(8):1291–1295 (**in Chinese**)

Liu CX, Yang LD, Li P (2009) Elastic-plastic analytical solution of deep buried circle tunnel considering stress redistribution. Eng Mech 26(2):16–20 (**in Chinese**)

Mhlongo SE (2023) Physical hazards of abandoned mines: a review of cases from south africa. Extract Indus Soc 15:101285. https://doi.org/10.1016/j.exis.2023.101285

Osgoui RR, Oreste P (2010) Elasto-plastic analytical model for the design of grouted bolts in a Hoek-Brown medium. Int J Numer Anal Methods Geomech 34(16):1651–1686. https://doi.org/10.1002/nag.823

Park KH, Kim YJ (2006) Analytical solution for a circular opening in an elastic–brittle–plastic rock. Int J Rock Mech Min Sci 43(4):616–622. https://doi.org/10.1016/j.ijrmms.2005.11.004

Reese D (2017) Utilities see hydroelectric potential in abandoned mines. https://wausaupilotandreview.com/2017/10/07/utilities-see-hydroelectric-potential-in-abandoned-mines. Accessed 7 Oct 2017

Rong CX, Cheng H (2004) Stability analysis of rocks around tunnel with ground water permeation. Chin J Rock Mech Eng 23(5):741–744 (**in Chinese**)

Salom AT, Kivinen S (2020) Closed and abandoned mines in namibia: a critical review of environmental impacts and constraints to rehabilitation. S Afr Geogr J 102(3):389–405. https://doi.org/10.1080/03736245.2019.1698450

Shin YJ, Song KI, Lee IM, Cho GC (2011) Interaction between tunnel supports and ground convergence—consideration of seepage forces. Int J Rock Mech Min Sci 48(3):394–405. https://doi.org/10.1016/j.ijrmms.2011.01.003

Sun ZY, Zhang DL, Fang Q (2019) The synergistic effect and design method of tunnel anchorage system. Eng Mech 36(5):53–75. https://doi.org/10.6052/j.issn.1000-4750.2018.03.0160. (**in Chinese**)

Wang JC, Kretschmann J, Li Y (2021) Reflections on resource utilization and sustainable development of closed coal mining areas. J Min Sci Technol 6(6):633–641. https://doi.org/10.19606/j.cnki.jmst.2021.06.001. (**in Chinese**)

Xu ZL (2016) Elasticity. Higher Education Press, Beijing, pp 73–80 (**in Chinese**)

Xue J, Hou X, Zhou J, Liu X, Guo Y (2022) Obstacle identification for the development of pumped hydro storage using abandoned mines: a novel multi-stage analysis framework. J Energy Storage 48:104022. https://doi.org/10.1016/j.est.2022.104022

Yang K, Fu Q, Yuan L, Liu Q, He X, Liu F (2023) Research on development demand and potential of pumped storage power plants combined with abandoned mines in china. J Energy Storage 63:106977. https://doi.org/10.1016/j.est.2023.106977

Yuan L, Yang K (2021) Further discussion on the scientific problems and countermeasures in the utilization of abandoned mines. J China Coal Soc 46(1):16–24. https://doi.org/10.13225/j.cnki.jccs.yg20.1966. (**in Chinese**)

Yuan L, Jiang YD, Wang K, Zhao YX, Hao XJ, Xu C (2018) Precision exploitation and utilization of closed /abandoned mine resources in China. J China Coal Soc 43(1):14–20. https://doi.org/10.13225/j.cnki.jccs.2017.1803. (**in Chinese**)

Yuan LJ, Li ZS, Wu SZ, Yang Z, Zhao ZH (2001) Engineering seepage mechanics and application. China Building Materials Press, Beijing, pp 33–38 (**in Chinese**)

Zareifard MR (2018) An analytical solution for design of pressure tunnels considering seepage loads. Appl Math Model 62:62–85. https://doi.org/10.1016/j.apm.2018.05.032

Zareifard MR, Fahimifar A (2015) Elastic–brittle–plastic analysis of circular deep underwater cavities in a Mohr-Coulomb rock mass considering seepage forces. Int J Geomech 15(5):04014077. https://doi.org/10.1061/(ASCE)GM.1943-5622.0000400

Zhang YJ, Zhang WQ (2013) An elastoplastic analytical solution for circular cavern considering combined thermo-hydro-mechanical action. Rock Soil Mech 34(S2):41–44. https://doi.org/10.16285/j.rsm.2013.s2.003. (**in Chinese**)

Zhao ZH, Wang WM, Tan YL, Wang LH (2016) Quantitative model of full section anchoring in thick soft rock tunnel. J China Coal Soc 41(7):1643–1650. https://doi.org/10.13225/j.cnki.jccs.2015.1313. (**in Chinese**)

Zhao Z, Sun W, Chen S, Feng Y, Wang W (2020) Displacement of surrounding rock in a deep circular hole considering double moduli and strength-stiffness degradation. Appl Math Mech 41(12):1847–1860. https://doi.org/10.1007/s10483-020-2665-9

Zhao Z, Li C, Meng Z, Liu H (2023) Theoretical analysis of grouting reinforcement of surrounding rock with strength drop in deep chamber. Acta Mech 234(10):4801–4819. https://doi.org/10.1007/s00707-023-03629-9

Zou J, Chen K, Pan Q (2018) An improved numerical approach in surrounding rock incorporating rockbolt effectiveness and seepage force. Acta Geotech 13(3):707–727. https://doi.org/10.1007/s11440-018-0635-8